Wnt/β-Catenin Signaling Regulates Telomerase in Stem Cells and Cancer Cells

Katrin Hoffmeyer *et al.*

Science **336**, 1549 (2012);
DOI: 10.1126/science.1218370

Wnt/β-Catenin Signaling Regulates Telomerase in Stem Cells and Cancer Cells

Katrin Hoffmeyer, Angelo Raggioli, Stefan Rudloff, Roman Anton,* Andreas Hierholzer, Ignacio Del Valle, Kerstin Hein, Riana Vogt, Rolf Kemler†

Telomerase activity controls telomere length and plays a pivotal role in stem cells, aging, and cancer. Here, we report a molecular link between Wnt/β-catenin signaling and the expression of the telomerase subunit *Tert*. β-Catenin–deficient mouse embryonic stem (ES) cells have short telomeres; conversely, ES cell expressing an activated form of β-catenin (β-cat$^{\Delta Ex3/+}$) have long telomeres. We show that β-catenin regulates *Tert* expression through the interaction with Klf4, a core component of the pluripotency transcriptional network. β-Catenin binds to the *Tert* promoter in a mouse intestinal tumor model and in human carcinoma cells. We uncover a previously unknown link between the stem cell and oncogenic potential whereby β-catenin regulates *Tert* expression, and thereby telomere length, which could be critical in human regenerative therapy and cancer.

Telomeres are specialized genomic structures that cap linear chromosomes and are essential for genome stability (*1*). Telomere length is controlled by the telomerase complex comprising an enzymatic subunit, TERT, and a RNA component, Terc (*2*). Embryonic and other stem cells have long telomeres, which become shorter during differentiation or aging but are stabilized again in tumorigenesis (*3*). The canonical Wnt signaling pathway plays a major role in regulating pluripotency in embryonic stem (ES) and adult stem cells from various tissues (*4*). β-Catenin is a central component of the Wnt pathway and forms a complex with members of the TCF family of transcription factors in the nucleus to control the transcription of target genes. Dysregulation of this pathway is frequently observed in human cancer (*5*). Here we show that TERT is directly regulated by β-catenin. Our results underline the cooperation between Wnt/β-catenin signaling and telomerase in the control of stem cell renewal.

β-Catenin regulates *Tert* expression in mouse ES cells. Comparing the expression profiles of wild-type and β-catenin–deficient (β-cat$^{-/-}$) ES cells, we found that *Tert*, but not *Terc*, mRNA was significantly reduced in the absence of β-catenin (Fig. 1A and fig. S1A). ES cells harboring a stabilized active form of β-catenin (β-cat$^{\Delta Ex3/+}$) had higher levels of *Tert* mRNA compared to wild-type cells (Fig. 1A). Those differences in *Tert* mRNA expression were reflected by TERT protein amounts in Western blot analysis (fig. S1C). Thus, altered levels of β-catenin affect *Tert* expression and may lead to differences in telomerase activity. Concordantly, telomerase activity was significantly increased in β-cat$^{\Delta Ex3/+}$ compared to the wild type and was reduced in β-cat$^{-/-}$ ES cells (Fig. 1B). Stimulation of wild-type ES cells with Wnt3a led to an increase in *Tert* expression (Fig. 1C). This supports recent findings that Wnt signaling may regulate Tert protein by sequestration of glycogen synthase kinase 3 (*6*). Knockdown of β-catenin by small interfering RNA (siRNA) reduced *Tert* expression and telomerase activity (Fig. 1D and fig. S1, D and E). Changes in *Tert* expression and telomerase activity resulted in different telomere lengths, with β-cat$^{-/-}$ cells having shortened telomeres (Fig. 1E). Telomeres in wild-type ES cells were on average 50 kb long; in β-cat$^{\Delta Ex3/+}$, 75 kb; and in β-cat$^{-/-}$ ES cells, 24 kb.

***Tert* is a direct target of β-catenin.** To gain insight into *Tert* transcriptional regulation by β-catenin, we performed luciferase reporter assays and chromatin immunoprecipitation (ChIP) experiments. *Tert* promoter fragments of 2.9 kb and 300 base pairs (bp) were equally active in wild-type ES cells (fig. S1F). The 300-bp fragment harbors binding sites for TCF and Klf4 (fig. S3C and S4G). β-Catenin was detected at the transcriptional start site (TSS) of *Tert* in wild-type ES cells by ChIP (Fig. 2A), which was further enhanced by the addition of Wnt3a (Fig. 2B). Binding of β-catenin to the TSS of *Tert* was also increased in β-cat$^{\Delta Ex3/+}$ cells, whereas no β-catenin was immunoprecipitated in β-cat$^{-/-}$ ES cells (Fig. 2A). The canonical β-catenin partners TCF3 and TCF4 were not detected at the *Tert* locus; however, TCF1 was enriched close to the TSS, even in β-cat$^{-/-}$ cells (figs. S2, A and B, and S3A). We postulate that TCF1 may act as a transcriptional repressor of *Tert*, as knockdown of TCF1 by siRNA and mutational analysis of the 300-bp promoter fragment suggest (fig. S3, B and D). In addition, no Oct3/4 binding at the *Tert* locus was observed (fig. S2C). c-Myc, a regulator of *Tert*, bound equally to the *Tert* promoter region in wild-type, β-cat$^{-/-}$, and β-cat$^{\Delta Ex3/+}$ cells, although c-Myc protein was reduced in β-cat$^{-/-}$ cells (fig. S2, D and E). Klf4 was of particular interest because of the conserved Klf4-binding site located at the TSS of the *Tert* promoter and because Klf4 contributes to the maintenance of telomerase activity in human cells (*7*). β-Catenin and Klf4 coimmunoprecipitate in wild-type ES cells (fig. S1G). Klf4 was identified at the *Tert* promoter by ChIP (Fig. 2C). Sequential ChIP revealed a Klf4/β-catenin complex at the *Tert* promoter (Fig. 2D). To study the relationship between β-catenin and Klf4, we inhibited the expression of Klf4 in wild-type ES cells with siRNAs with or without Wnt3a stimulation (Fig. 2E and fig. S4). The accumulation of β-catenin on the *Tert* promoter upon Wnt3a stimulation was severely reduced after Klf4 knockdown. Therefore, Klf4 is required for β-catenin to localize to the *Tert* promoter. However, Klf4 alone was insufficient to drive *Tert* expression, as Klf4 was bound to the *Tert* promoter in β-cat$^{-/-}$ cells, where *Tert* expression is low (Fig. 2C). Furthermore, whereas re-expression of β-catenin in β-cat$^{-/-}$ cells led to an increase in *Tert* mRNA level, overexpression of Klf4 did not (Fig. 2F). Therefore, recruitment of β-catenin is necessary for *Tert* transcription in mouse ES cells, and Klf4 promotes this binding.

β-Catenin regulates *Tert* promoter activity. Supporting the role of β-catenin in *Tert* promoter activation, RNA polymerase II (Pol II), Pol II Ser5p (active Pol II), and the active trimethylated lysine-4 on histone-3 (H3K4me3) were detected at the *Tert* promoter in wild-type and β-cat$^{\Delta Ex3/+}$, but not in β-cat$^{-/-}$, cells (Fig. 3, A and B, and fig. S5B). Both Pol II and H3K4me3 were reestablished at the *Tert* promoter in β-cat$^{-/-}$ cells upon transfection with constitutively active β-catenin (Fig. 3C and fig. S6A). These results demonstrate that β-catenin is required for *Tert* promoter activation. We identified two members of the trithorax group (TrxG) proteins, Ash2l and Setd1a (*8*), the latter of which exhibited histone methyltransferase (HMT) activity at the TSS of the *Tert* promoter in ES cells. The localization of Ash2l and Setd1a at the *Tert* promoter depended on β-catenin, was not detected in β-cat$^{-/-}$ ES cells, and was enhanced in β-cat$^{\Delta Ex3/+}$ ES cells (Fig. 3, E and F, and figs. S5 and 6). Transfection experiments in human embryonic kidney 293 (HEK293) cells followed by coimmunoprecipitation revealed an association of β-catenin with Ash2l and Setd1a (Fig. 3D). These data suggest that β-catenin actively recruits HMTs to regulate the chromatin modifications required for the initiation of *Tert* transcription.

β-Catenin binds to the *Tert* promoter in adult stem cells. Next, we examined β-catenin at the *Tert* promoter in adult stem cells. The crypt of

Department of Molecular Embryology, Max Planck Institute of Immunobiology and Epigenetics, Stuebeweg 51, D-79108 Freiburg, Germany.

*Present address: Institute of Pharmacology and Toxicology, Rheinische Friedrich-Wilhelms-University of Bonn, Sigmund-Freud-Strasse 25, D-53127 Bonn, Germany.

†To whom correspondence should be addressed. E-mail: kemler@immunbio.mpg.de

the small intestine contains stem cells; the villus contains more differentiated epithelial cells (*9*). β-Catenin bound to the TSS of *Tert* was only detected in the crypt cell fraction (Fig. 4A). This was further validated by β-catenin ChIP from isolated Lgr5-positive stem cells using Lgr5::GFP (green fluorescent protein) reporter mice (Fig. 4B) and in organoids from crypt cell cultures (fig. S7D). β-Catenin binding to the *Tert* promoter (Fig. 4A) correlated with Pol II binding (fig. S9A) and different expression levels of *Tert* in the crypt versus villus fractions (Fig. 5B).

To determine whether our findings were relevant in other stem or progenitor cells, we made use of the Hes5::GFP reporter mouse (*10*) and analyzed primary neurospheres. In isolated Hes5::GFP neural stem cells, as well as in primary neurospheres, β-catenin was enriched at the TSS of the *Tert* promoter (Fig. 4C). Deletion of β-catenin by adeno-mediated cre resulted in a reduction in *Tert* mRNA expression and abolished β-catenin binding to the *Tert* promoter (Fig. 4C and fig. S10).

β-Catenin regulates Tert expression in human cancer cells. Aberrant nuclear activation of β-catenin in cells of the villus leads to increased cell proliferation and the formation of polyps

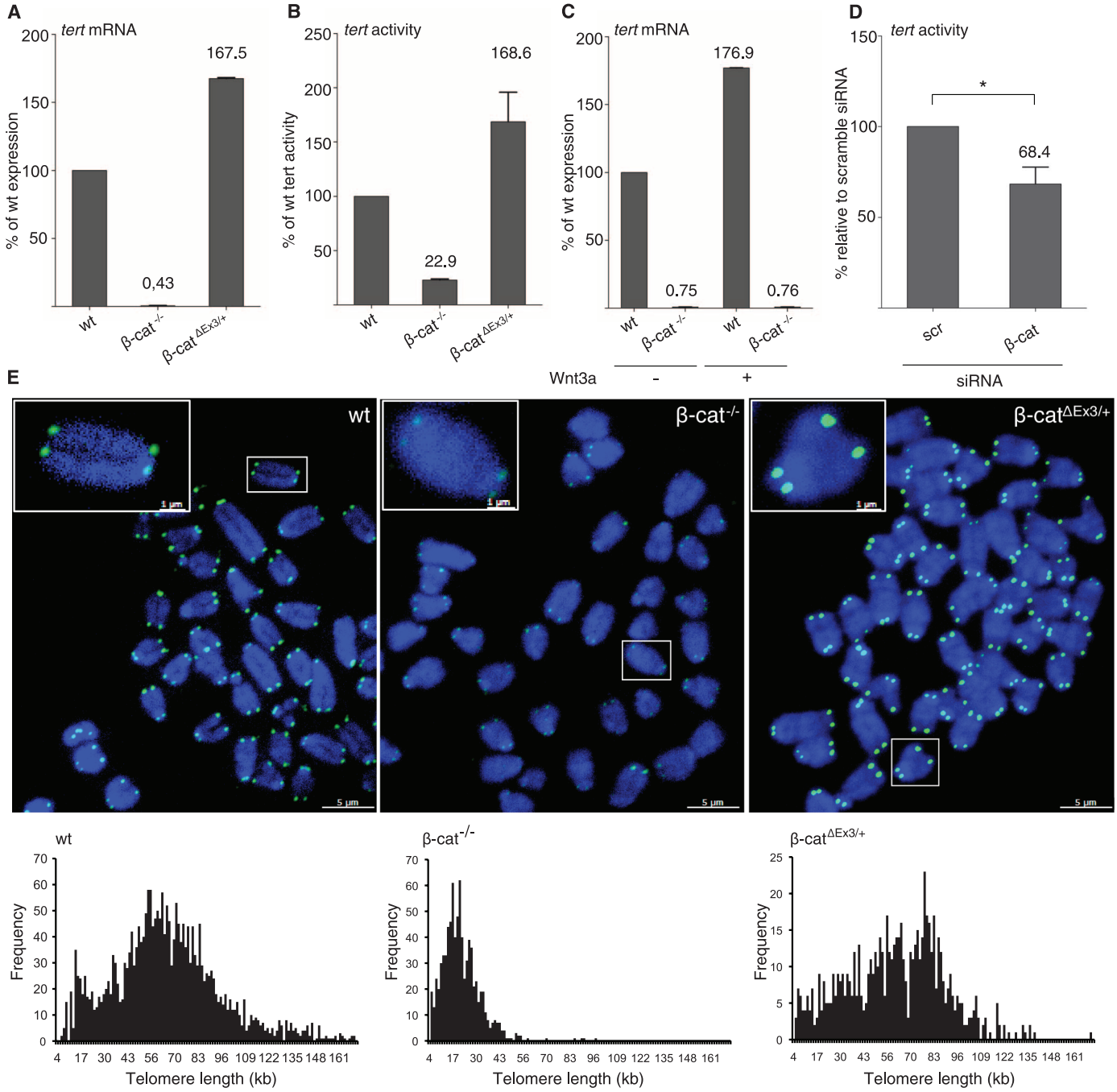

Fig. 1. β-Catenin regulates *Tert* mRNA expression, telomerase activity, and telomere length in genetically modified ES cells. (**A**) Quantitative polymerase chain reaction analysis of *Tert* mRNA. (**B**) Telomerase activity. (**C** and **D**) In wild-type (wt) ES cells Wnt3a induces *Tert* expression, whereas knockdown of β-catenin by siRNA reduces *Tert* expression and activity (fig. S1). (**E**) Telomere length determined by quantitative fluorescence in situ hybridization analysis and TFL-Telo software in comparison to reference cell lines. ($n = 7$, $^*P < 0.05$).

and adenomatous lesions (*11*). We established a mouse model to analyze *Tert* in hyperplastic lesions in the small intestine by the conditional activation of one β-catenin gain-of-function allele (villin-creERT × β-cat$^{Ex3fl/+}$). Stabilized β-catenin was detected in β-cat$^{\Delta Ex3/+}$ crypt and villus cells (Fig. 5A). In the β-cat$^{\Delta Ex3/+}$ intestine, hyperproliferative cells and induced expression of β-catenin target genes, such as those encoding c-Myc, Axin2, and CD44, were detected in the epithelia all along the crypt-villus axis (Fig. 5A and fig. S8A). Expansion of the Paneth cell–specific marker, lysozyme, and CD44 was also observed in the villi (fig. S8B). Expression of *Tert* (Fig. 5B), *Lgr5*, and *Klf4* mRNAs (fig.S8A) was induced in the villus fraction of mutants. Concordantly, β-catenin and Pol II binding was increased at the TSS of *Tert* in villus cells (Fig. 5C and fig. S9B). These results provide strong in vivo evidence for the transcriptional regulation of *Tert* by β-catenin.

Finally, we examined whether the regulation of *Tert* expression by β-catenin may also be important in human cancer. We studied the human embryonal carcinoma cell line NTera2 and the human colorectal carcinoma cell line SW480, the latter exhibiting increased amounts of cytoplasmic and nuclear β-catenin due to mutations in adenomatous polyposis coli (APC). β-Catenin was present at the TSS of h*TERT* (Fig. 5D), and knockdown of β-catenin by siRNA

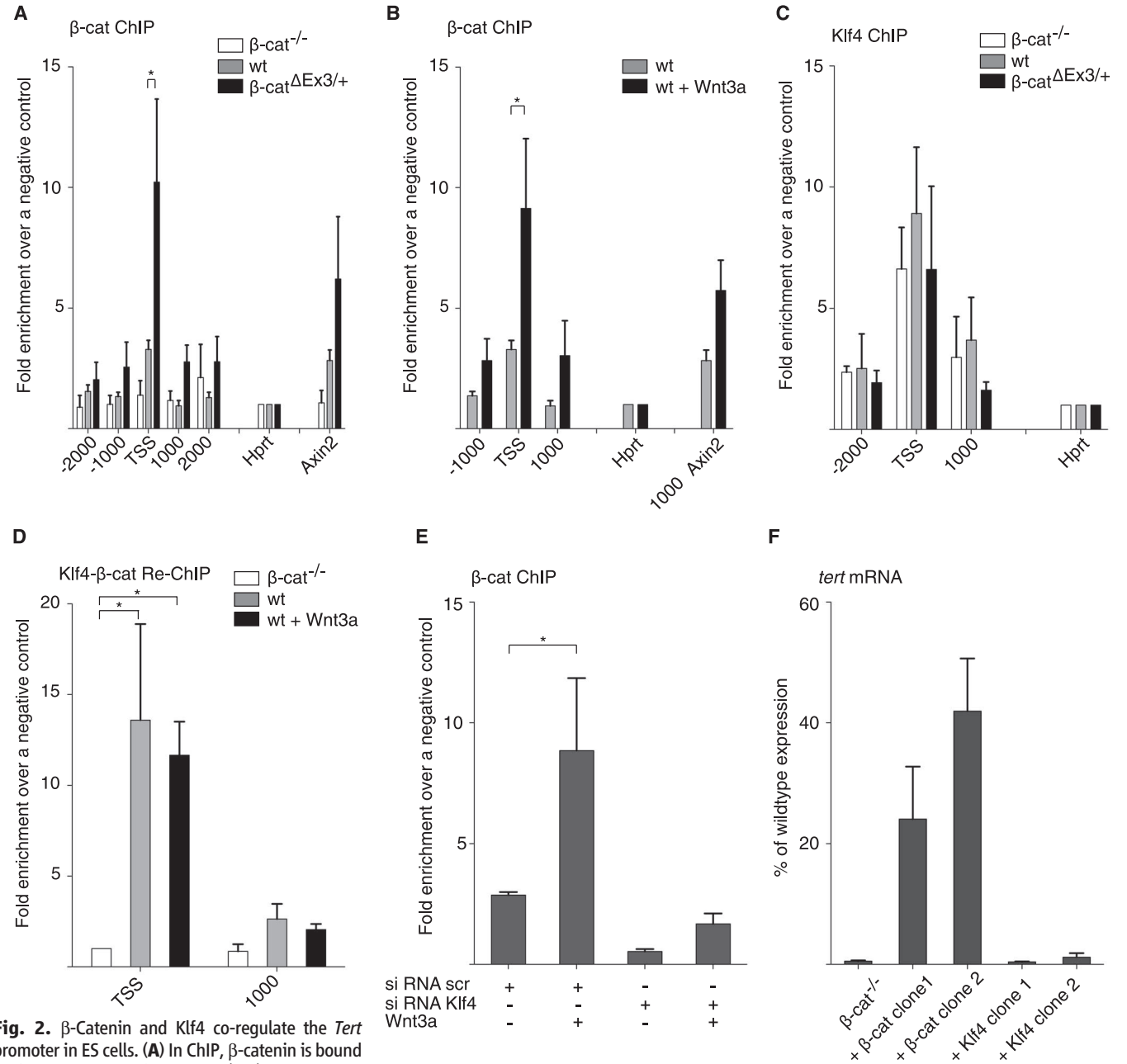

Fig. 2. β-Catenin and Klf4 co-regulate the *Tert* promoter in ES cells. (**A**) In ChIP, β-catenin is bound at the transcriptional start site (TSS) of *Tert* in wt and β-cat$^{\Delta Ex3/+}$ but not in β-cat$^{-/-}$ ES cells. (**B**) Enrichment of β-catenin at the TSS of *Tert* after stimulation with Wnt3a. (**C**) In ChIP, Klf4 is localized at the TSS of *Tert* in wt, β-cat$^{\Delta Ex3/+}$, and β-cat$^{-/-}$ cells. (**D**) Re-ChIP, anti-Klf4 followed by anti–β-catenin, demonstrating that both form a complex at the *Tert* promoter. (**E**) Wild-type ES cells transfected with siRNA for Klf4 (48 hours) were cultivated with (+) or without (–) Wnt3a (12 hours). β-Catenin binding to the *Tert* promoter was analyzed by ChIP (fig. S4). (**F**) β-cat$^{-/-}$ cells were stably transfected with β-catenin or Klf4, and two independent clones were analyzed. Only overexpression of β-catenin resulted in reexpression of *Tert* mRNA. Axin2 was used as a positive control region and hypoxanthine phosphoribosyltransferase (Hprt) as a negative control region in ChIP experiments. (*P < 0.05, table S3).

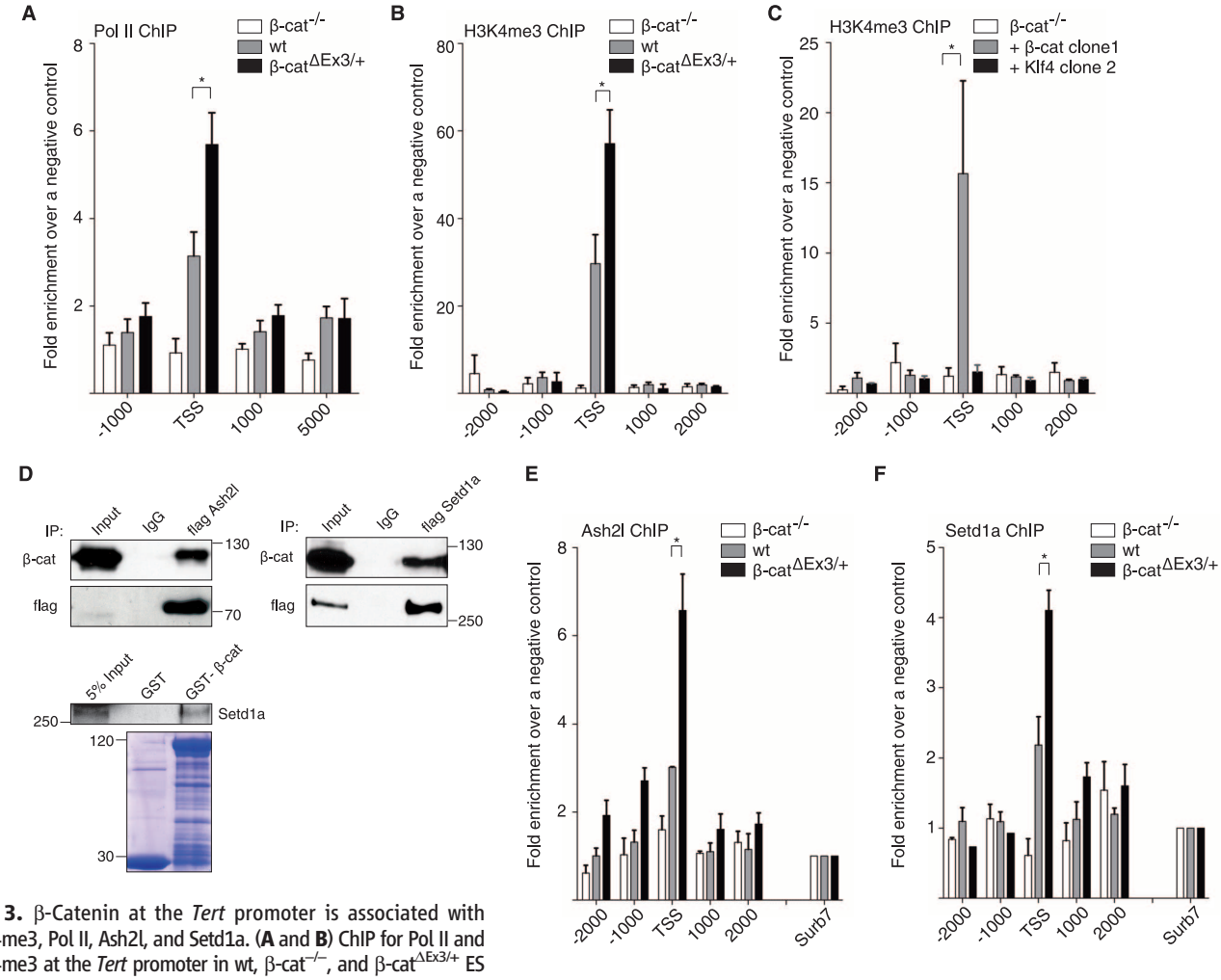

Fig. 3. β-Catenin at the *Tert* promoter is associated with H3K4me3, Pol II, Ash2l, and Setd1a. (**A** and **B**) ChIP for Pol II and H3K4me3 at the *Tert* promoter in wt, β-cat$^{-/-}$, and β-cat$^{\Delta Ex3/+}$ ES cells (fig. S5). (**C**) ChIP for H3K4me3 and Pol II (fig. S6A) at the *Tert* promoter in β-cat$^{-/-}$ cells overexpressing β-catenin or Klf4. (**D**) (Upper panels) β-Catenin and Setd1a (right) and β-catenin and Ash2l (left) association in HEK293 cells, as shown by coimmunoprecipitation (co-IP). In vitro–translated Setd1a associates with glutathione *S*-transferase (GST)–β-catenin (lower panel). (**E** and **F**) Ash2l and Setd1a binding to the *Tert* promoter correlates with the β-catenin levels in wt, β-cat$^{-/-}$, and β-cat$^{\Delta Ex3/+}$ ES cells as assessed by ChIP. Surb7, negative control. (*$P < 0.05$, table S3).

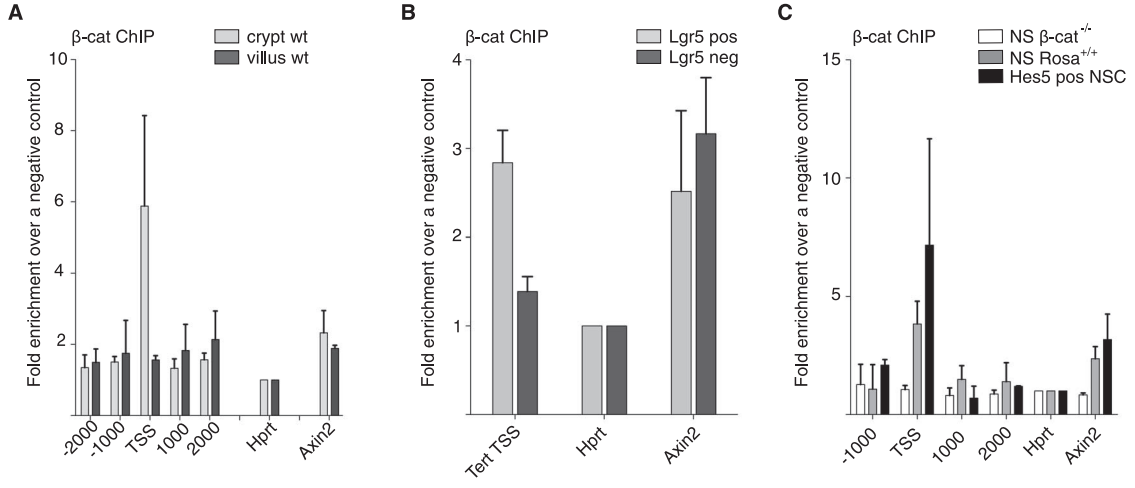

Fig. 4. Binding of β-Catenin at the *Tert* promoter in adult stem cells. (**A**) Mouse small intestines were separated into crypt and villus fractions and subjected to ChIP. β-Catenin at the TSS of *Tert* was detected only in the crypt cell compartment. (**B**) Lgr5-positive stem cells were isolated from Lgr5::GFP reporter mice by fluorescence-activated cell sorting (FACS) and subjected to ChIP. (**C**) The Hes5::GFP reporter mouse was used to isolate neural stem cells by FACS. ChIP for β-catenin in isolated Hes5::GFP neural stem cells (NSC) and in neurospheres (NS) infected with adeno-cre revealed binding of β-catenin at the *Tert* promoter, which is abolished in neurospheres when β-catenin is deleted.

reduced h*TERT* mRNA levels in both cell lines (Fig. 5E and fig. S11C).

***Tert* is a β-catenin target.** By regulating *Tert* expression, β-catenin may assure the correct telomere length in stem cells, promoting their genomic stability and maintenance. Telomerase is directly involved in the regulation of Wnt/β-catenin target genes (*12*). Our findings indicate a regulatory loop between β-catenin and *Tert* expression. In mouse ES cells, we identified Klf4 as a partner of β-catenin in the regulation of *Tert* expression, but TCF1 may also be involved. The transcriptional regulation of *Tert* is very likely complex and combinatorial, and β-catenin may regulate *Tert* expression in other stem cell compartments in concert with other transcription factors. Clearly, in the absence of β-catenin, the *Tert* gene is silenced, but *Tert* transcription is initiated when β-catenin is recruited to the *Tert* promoter. We show that the initiation of *Tert* transcription is accompanied by H3K4 trimethylation at the promoter, and we identified the lysine methyltransferase Setd1a as an interaction partner of β-catenin. Our results suggest that β-catenin recruits HMTs to initiate *Tert* transcription, which supports the increasingly recognized role of β-catenin in chromatin remodeling (*13*).

Furthermore, we show the localization of β-catenin at the *Tert* promoter to adult mouse stem cells and to human cancer cell lines, supporting

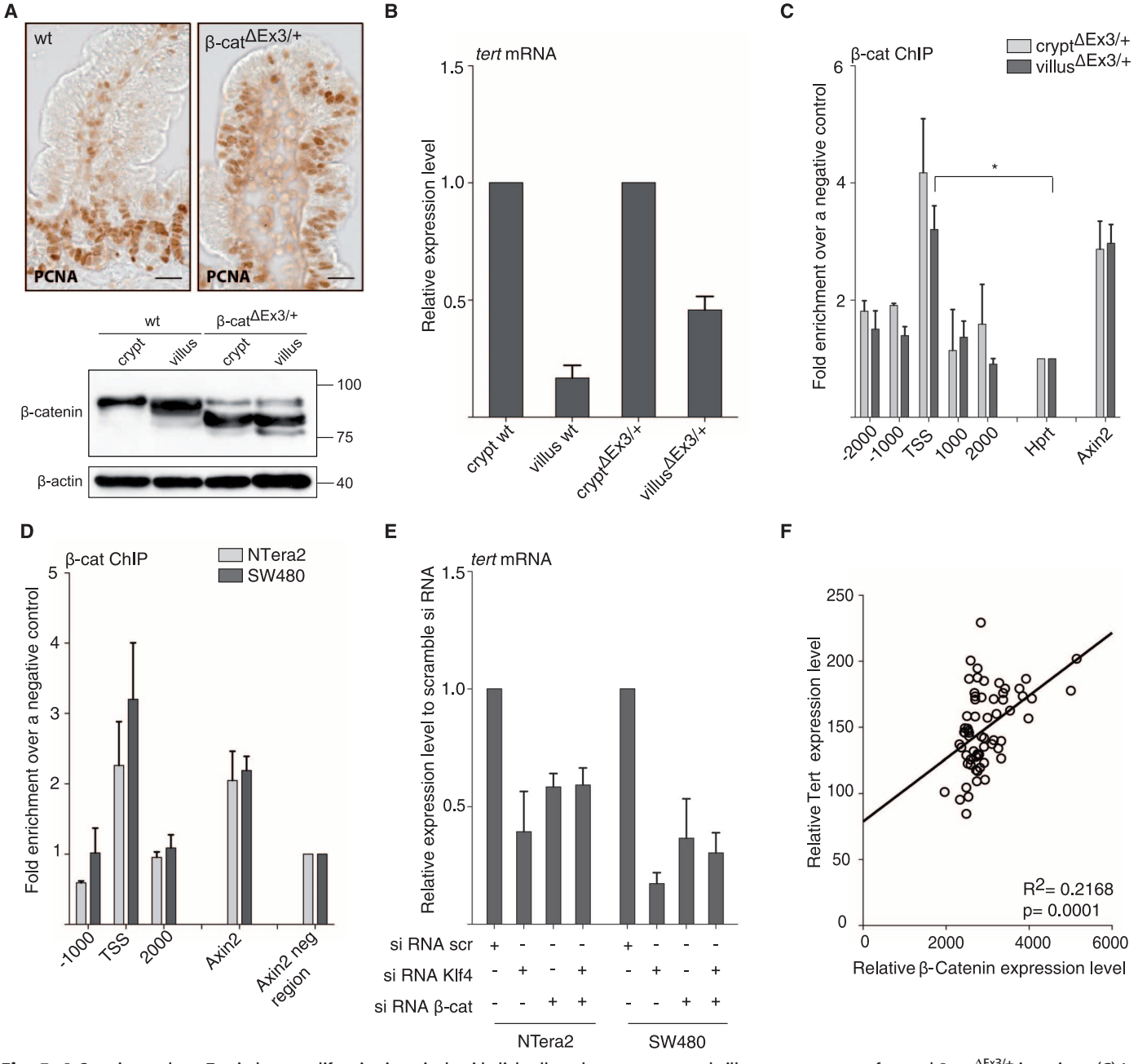

Fig. 5. β-Catenin regulates *Tert* in hyperproliferative intestinal epithelial cells and in human cancer cell lines. (**A**) Hyperplastic lesions in the intestine were induced by the stabilized active form of β-catenin (Villin-cre ERT × β-cat$^{Exf13/+}$), which resulted in hyperproliferative cells all along the crypt-villus axis, as seen by staining for proliferating cell nuclear antigen (PCNA) (upper panels). The stabilized form of β-catenin (β-cat$^{\Delta Ex3/+}$) is smaller in size and equally expressed in the crypt and villus fractions (lower panels). (**B**) Comparison of *Tert* mRNA between crypt and villus compartments of wt and β-cat$^{\Delta Ex3/+}$ intestines. (**C**) In β-cat$^{\Delta Ex3/+}$ intestines, β-catenin is bound to the TSS of *Tert* in crypt and villus cell compartments (*$P < 0.05$, table S3). (**D**) In human NTera2 and SW480 cells, β-catenin is bound at the TSS of h*TERT*, as detected by ChIP. (**E**) siRNA-mediated knockdown of β-catenin and Klf4 reduces expression of *TERT* mRNA. (**F**) Significant correlation between *TERT* and β-catenin expression in human colon cancer samples; $P < 0.0001$, $R^2 = 0.21068$ (for details, see fig. S11A).

the notion that the regulation of *Tert* by β-catenin is a general biological feature. Our mouse model (villin-creERT × β-cat$^{Ex3fl/+}$) provides in vivo evidence that the aberrant activation of β-catenin in the epithelium of the small intestine leads to *Tert* expression and binding of β-catenin to the *Tert* promoter. Exon 3 encodes phosphorylation sites important for β-catenin protein stability (*14*), and these sites are frequently mutated in human colorectal and other cancers (*15*). It is notable that in human colorectal cancers, high *Tert* and β-catenin expression are significantly correlated ($P = 0.0001$), as taken from publicly available microarray data sets (*16*) (Fig. 5F and fig. S11A).

Conclusion. By identifying *Tert* as a target gene of β-catenin, we demonstrate a link between these two key regulators in stem cell biology and cancer. From the results presented here, we propose that mutations in β-catenin can lead to an enhanced *Tert* expression in human cancer, which results in the stabilization of telomeres, one of the hallmarks of tumorigenesis.

References and Notes

1. M. A. Blasco, *Nat. Rev. Genet.* **8**, 299 (2007).
2. H. D. Wyatt, S. C. West, T. L. Beattie, *Nucleic Acids Res.* **38**, 5609 (2010).
3. T. Miura, M. P. Mattson, M. S. Rao, *Aging Cell* **3**, 333 (2004).
4. S. Y. Sokol, *Development* **138**, 4341 (2011).
5. T. Reya, H. Clevers, *Nature* **434**, 843 (2005).
6. V. F. Taelman *et al.*, *Cell* **143**, 1136 (2010).
7. C. W. Wong *et al.*, *Stem Cells* **28**, 1510 (2010).
8. B. Schuettengruber, A. M. Martinez, N. Iovino, G. Cavalli, *Nat. Rev. Mol. Cell Biol.* **12**, 799 (2011).
9. T. Sato *et al.*, *Nature* **459**, 262 (2009).
10. O. Basak, V. Taylor, *Eur. J. Neurosci.* **25**, 1006 (2007).
11. N. Harada *et al.*, *EMBO J.* **18**, 5931 (1999).
12. J. I. Park *et al.*, *Nature* **460**, 66 (2009).
13. C. Mosimann, G. Hausmann, K. Basler, *Nat. Rev. Mol. Cell Biol.* **10**, 276 (2009).
14. H. Aberle, A. Bauer, J. Stappert, A. Kispert, R. Kemler, *EMBO J.* **16**, 3797 (1997).
15. V. Korinek *et al.*, *Science* **275**, 1784 (1997).
16. S. Kaiser *et al.*, *Genome Biol.* **8**, R131 (2007).

Acknowledgments: We thank H. H. Ng (Singapore) for the antibody against Klf4, I. Horikawa (NIH) for the 300-bp promoter construct, and J.-H. Lee (Indiana University) for Ash2l and Setd1a expression vectors. We thank E. M. Varela and M. Blasco (Madrid) for advice and reagents for the Q-fish analysis and for antibodies against Tert. We are grateful to M. M. Taketo (Kyoto) and to S. Robine (Paris) for providing mutant mice. We thank S. Lugert for advice on neurosphere cultures, J. Volkind for technical assistance, V. Taylor and D. Junghans for discussion and critical reading, and R. Schneider for typing of the manuscript. K.H. and A.R. are members of the International Max Planck Research School for Molecular and Cellular Biology (IMPRS-MCB). This work was supported by the Max Planck Society. The authors declare no financial interests.

Supplementary Materials

www.sciencemag.org/cgi/content/full/336/6088/1549/DC1
Materials and Methods
Figs. S1 to S11
Tables S1 to S3
References (*17*–*25*)

22 December 2011; accepted 9 April 2012
10.1126/science.1218370

REPORTS

A Sharp Peak of the Zero-Temperature Penetration Depth at Optimal Composition in $BaFe_2(As_{1-x}P_x)_2$

K. Hashimoto,[1]* K. Cho,[2,3] T. Shibauchi,[1]† S. Kasahara,[1,4] Y. Mizukami,[1] R. Katsumata,[1] Y. Tsuruhara,[1] T. Terashima,[4] H. Ikeda,[1] M. A. Tanatar,[2] H. Kitano,[5] N. Salovich,[6] R. W. Giannetta,[6] P. Walmsley,[7] A. Carrington,[7] R. Prozorov,[2,3] Y. Matsuda[1]†

In a superconductor, the ratio of the carrier density, n, to its effective mass, m^*, is a fundamental property directly reflecting the length scale of the superfluid flow, the London penetration depth, λ_L. In two-dimensional systems, this ratio n/m^* ($\sim 1/\lambda_L^2$) determines the effective Fermi temperature, T_F. We report a sharp peak in the x-dependence of λ_L at zero temperature in clean samples of $BaFe_2(As_{1-x}P_x)_2$ at the optimum composition $x = 0.30$, where the superconducting transition temperature T_c reaches a maximum of 30 kelvin. This structure may arise from quantum fluctuations associated with a quantum critical point. The ratio of T_c/T_F at $x = 0.30$ is enhanced, implying a possible crossover toward the Bose-Einstein condensate limit driven by quantum criticality.

In two families of high-temperature superconductors, cuprates and iron-pnictides, superconductivity emerges in close proximity to an antiferromagnetically ordered state, and the critical temperature, T_c, has a dome-shaped dependence on doping or pressure (*1*–*3*). What happens inside this superconducting dome is still a matter of debate (*3*–*5*). In particular, elucidating whether a quantum critical point (QCP) is hidden inside it (Fig. 1, A and B) may be key to understanding high-T_c superconductivity (*5*, *6*). A QCP marks the position of a quantum phase transition (QPT), a zero-temperature phase transition driven by quantum fluctuations (*7*).

The London penetration depth, λ_L, is a property that may be measured at low temperature in the superconducting state to probe the electronic structure of the material and to look for signatures of a QCP. The absolute value of λ_L in the zero-temperature limit immediately gives the superfluid density $\lambda_L^{-2}(0) = \mu_0 e^2 \Sigma_i n_i/m_i^*$, which is a direct probe of the superconducting state; here, m_i^* and n_i are the effective mass and concentration of the superconducting carriers in band i, respectively (*8*). Measurements on high-quality crystals are necessary because impurities and inhomogeneity may otherwise wipe out the signatures of the QPT. Another advantage of this approach is that it does not require the application of a strong magnetic field, which may induce a different QCP or shift the zero-field QCP (*9*).

$BaFe_2(As_{1-x}P_x)_2$ is a particularly suitable system for penetration depth measurements because, in contrast to most other Fe-based superconductors, very clean (*10*) and homogeneous crystals of the whole composition series can be grown (*11*). In this system, the isovalent substitution of P for As in the parent compound $BaFe_2As_2$ offers an elegant way to suppress magnetism and induce superconductivity (*11*). Non–Fermi liquid properties are apparent in the normal state above the superconducting dome (Fig. 2A) (*11*, *12*), and de Haas–van Alphen (dHvA) oscillations (*10*) have been observed over a wide x range, including the superconducting compositions, giving detailed information on the electronic structure. Because P and As are isoelectronic, the system remains compensated for all values of x (i.e., volumes of the electron and hole Fermi surfaces are equal).

As discussed in (*10*), the normal-state electronic structure of $BaFe_2(As_{1-x}P_x)_2$ determined by dHvA experiments is significantly modified from that predicted by conventional density functional theory (DFT) band structure calculations. Figure 2A shows the composition evolution of the effective mass, m^*, normalized by the free

[1]Department of Physics, Kyoto University, Kyoto 606-8502, Japan. [2]The Ames Laboratory, Ames, IA 5001, USA. [3]Department of Physics and Astronomy, Iowa State University, Ames, IA 50011, USA. [4]Research Center for Low Temperature and Materials Sciences, Kyoto University, Kyoto 606-8501, Japan. [5]Department of Physics and Mathematics, Aoyama Gakuin University, 5-10-1 Fuchinobe, Chuo-ku, Sagamihara, Kanagawa 252-5258, Japan. [6]Loomis Laboratory of Physics, University of Illinois at Urbana-Champaign, 1110 West Green Street, Urbana, IL 61801, USA. [7]H. H. Wills Physics Laboratory, University of Bristol, Tyndall Avenue, Bristol, UK.

*Present address: Institute for Materials Research, Tohoku University, Sendai 980-8577, Japan.
†To whom correspondence should be addressed. E-mail: matsuda@scphys.kyoto-u.ac.jp (Y.M.); shibauchi@scphys.kyoto-u.ac.jp (T.S.)